RBMO

ELSEVIER

ARTICLE

MUC20 expression marks the receptive phase of the human endometrium

BIOGRAPHY

Leading author Artjom Stepanjuk graduated *cum laude* with a Master of Science degree in Molecular and Cell Biology from the University of Tartu, Estonia. Now is working on his PhD under the supervision of professor Andres Salumets and associated professor Sulev Ingerpuu at the same university.

Artjom Stepanjuk[1], Mariann Koel[1,2], Martin Pook[1], Merli Saare[2,3], Kersti Jääger[2], Maire Peters[2,3], Kaarel Krjutškov[2,4], Sulev Ingerpuu[1], Andres Salumets[2,3,5,6,*]

KEY MESSAGE

The main source of mucin MUC20 mRNA and protein in the human endometrium is an epithelial compartment. MUC20 expression is cycle-dependent and can be considered as a new potential marker candidate of receptive endometrium that may prove useful for IVF patients after clinical validation.

ABSTRACT

Research question: How does mucin MUC20 expression change during the menstrual cycle in different cell types of human endometrium?

Design: Study involved examination of MUC20 expression in two previously published RNA-seq datasets in whole endometrial tissue (n = 10), sorted endometrial epithelial (n = 44) or stromal (n = 42) cell samples. RNA-Seq results were validated by quantitative reverse transcription polymerase chain reaction (qRT-PCR) in whole tissue (n = 10), sorted epithelial (n = 17) and stromal (n = 17) cell samples. MUC20 protein localization and expression were analysed in human endometrium by immunohistochemical analysis of intact endometrial tissue (n = 6) and also Western blot of cultured stromal and epithelial cells (n = 2).

Results: MUC20 is differentially expressed in the endometrium between the pre-receptive and receptive phases. We show that MUC20 is predominantly expressed by epithelial cells of the receptive endometrium, both at the mRNA (RNA-Seq, P = 0.005; qRT-PCR, P = 0.039) and protein levels (Western blot; immunohistochemistry, P = 0.029).

Conclusion: Our results indicate MUC20 as a novel marker of mid-secretory endometrial biology. We propose a model of MUC20 function in the hepatocyte growth factor (HGF)-activated mesenchymal–epithelial transition (MET) receptor signalling specifically in the receptive phase. Further investigations should reveal the precise function of MUC20 in human endometrium and the possible connection between MUC20 and HGF-activated MET receptor signalling. MUC20 could potentially be included in the list of endometrial receptivity markers after further clinical validation.

[1] Institute of Molecular and Cell Biology, University of Tartu, Riia 23, Tartu 51010, Estonia
[2] Competence Centre on Health Technologies, Tiigi 61b, Tartu 50410, Estonia
[3] Department of Obstetrics and Gynecology, Institute of Clinical Medicine, University of Tartu, L. Puusepa 8, Tartu 50406, Estonia
[4] Research Program of Molecular Neurology, Research Programs Unit, University of Helsinki, and Folkhälsan Institute of Genetics, Haartmaninkatu 8, Helsinki 00290, Finland
[5] Department of Biomedicine, Institute of Biomedicine and Translational Medicine, University of Tartu, Ravila 19, Tartu 50411, Estonia
[6] Department of Obstetrics and Gynecology, University of Helsinki and Helsinki University Hospital, Haartmaninkatu 2, Helsinki 00014, Finland

KEYWORDS

MUC20
Endometrium
Implantation
Mucin
Receptivity
Window of implantation

*Corresponding author. E-mail address: andres.salumets@ccht.ee (A Salumets). https://doi.org/10.1016/j.rbmo.2019.05.004
1472-6483/
Declaration: The authors report no financial or commercial conflicts of interest.

INTRODUCTION

Successful implantation of a blastocyst to the maternal endometrium is one of the key events during embryonic development. Endometrial tissue cells that respond to hormonal regulation interact with the blastocyst only during a short period during normal endometrial maturation (5–6 days after fertilization) (*Hertig et al., 1956*), which is referred to as a window of implantation (WOI) or a receptivity phase (*Psychoyos, 1986*). The surface of the endometrial epithelium is the site where the first molecular interactions occur between the trophoblast cells of the implanting embryo and the maternal organism (*Enders et al., 1983*). The molecular mechanisms of the embryo implantation process, however, are still incompletely understood. Although assisted reproductive technologies have been widely used over the past decades, the rate of successful pregnancies among patients who had passed IVF procedure has not risen. The ability to define the WOI more precisely could significantly improve the pregnancy rate of the IVF procedure.

Different approaches have been implemented to estimate the WOI in the human endometrium, including dating of endometrial development based on morphological parameters of endometrial tissue biopsies (*Noyes et al., 1950*), immunohistological dating with integrated expression scoring of previously known receptivity biomarkers, e.g. αVβ3 integrin (*Germeyer et al., 2014*), and, more recently, transcriptomics-based analysis of the differences between pre-receptive and receptive endometrium (*Carson et al., 2002; Talbi et al., 2006; Haouzi et al., 2009; Sha et al., 2011; Hu et al., 2014*). The commercial endometrial receptivity array test (ERA) uses the expression profiling of 238 pre-defined genes and is currently used in clinical diagnostics (*Díaz-Gimeno et al., 2011*). Transcriptome-based studies typically suffer from the small overlap between different studies (*Altmäe et al., 2014*), which can be increased by improved meta-analysis that has the potential to reveal the signature of human endometrial receptivity (*Altmäe et al., 2017*). New molecular markers, however, are needed for more accurate dating of WOI and a deeper understanding of the receptivity mechanisms in human endometrium.

Mucins are integral components of mucosal surfaces all over the body, having a high variety of functions from the physical protection and lubrication of the epithelial layers to the molecular modulation of immunity and cell signalling (*Hattrup and Gendler, 2008; Corfield, 2015*). The mucin barrier is hormonally regulated during the menstrual cycle in many mammalian species, including humans (*Thathiah and Carson, 2002*). Mucins form a diverse family of 19 highly glycosylated proteins, which are divided into two groups: secreted, and membrane-associated or membrane-tethered types. The uterine membrane-tethered mucins play an essential role during embryo implantation (*Thathiah and Carson, 2002*). Despite the potential role of endometrial mucins in the regulation of receptivity, the only mucin that has been intensively studied in the human endometrium is MUC1 (*Aplin et al., 1994; Hey et al., 1994*). Only a few studies have mentioned MUC4 and MUC16 in the context of human endometrial receptivity (*Koscinski et al., 2006; Gipson et al., 2008; Dharmaraj et al., 2014*).

One of the mucins, MUC20, differs considerably from other members of the mucin family, both by a relatively small size and a low level of glycosylation. This contrasts with other membrane-tethered mucins that are highly glycosylated and can protrude from the cell membrane up to hundreds of nanometers, and form the glycocalyx (*Corfield, 2017*). MUC20, on the other hand, has an untypically long cytoplasmic tail (*Higuchi et al., 2004a*). MUC20 was described relatively recently, and its functions in cell physiology are not well known (*Higuchi et al., 2004b*). In this study, we set out to determine the expression of MUC20 precisely in different endometrial cell types in the pre-receptive and receptive phases.

MATERIALS AND METHODS

Study participants

The study was approved (19 December 2012) and prolonged (18 December 2017) by the Research Ethics Committee of the University of Tartu (protocol No 221/M-31; prolongation protocol No 276/M-15). Written informed consent was obtained from all participants. Endometrial biopsies were obtained from healthy volunteers at fertile age (≤35 years) with normal body mass index (BMI) (within a range of 19–25 kg/m^2). All women selected for the study had a regular menstrual cycle, were clinically examined by ultrasound for the absence of visible pelvic pathologies and polycystic ovary syndrome, and had no symptoms or complaints of endometriosis. The levels of testosterone and prolactin, measured from the blood plasma, corresponded to the normal values of reproductive age women. The level of progesterone measured from the blood plasma samples collected in the mid-secretory phase of the menstrual cycle corresponded to the expected levels at that cycle phase. The women were non-smokers, were not taking any hormonal treatments for 3 months before the study, had no previous infertility record, and had at least one live-born child. Endometrial biopsies were obtained using a Pipelle catheter (Laboratoire CCD, Paris, France) on day 2 and 8 after the LH surge (LH+2 and LH+8) within the same natural cycle. Menstrual cycle dating was confirmed by combining menstrual cycle history and LH peak estimation by the BabyTime LH urine cassette (Pharmanova, Beograd, Serbia), vaginal ultrasound and histological evaluation of biopsy according to Noyes' criteria (*Noyes et al., 1950*). Altogether, 10 women were recruited in whom *MUC1* and *MUC20* expression levels were detected in whole endometrial tissue biopsies; 26 women were recruited in whom MUC1 and MUC20 expression levels were identified in sorted endometrial stromal and epithelial. Immunohistological evaluation was carried out in six additional women.

Western blot analysis was carried out on cultured primary epithelial and stromal cells obtained from two women. For isolation of primary cultures of endometrial epithelial and stromal cells, two separate biopsies were obtained. The first endometrial biopsy (proliferative phase, menstrual cycle day 12) was obtained from one 44-year-old woman (reproductive history: three pregnancies and three deliveries) with endometriosis (stage 3) undergoing laparoscopy at the Tartu University Hospital Women's Clinic, Tartu, Estonia. The woman had a regular menstrual cycle (28 ± 5 days), BMI 21 kg/m^2 and used no hormonal medications during the previous 3 months before laparoscopy. A second endometrial biopsy (early secretory phase, menstrual cycle day 19) was obtained from one 35-year-old woman

(reproductive history: one pregnancy and one delivery) with secondary infertility undergoing laparoscopy at the Tartu University Hospital Women's Clinic, Tartu, Estonia. No sign of pelvic abnormalities (no adhesions, normal size of uterus and ovaries) or endometriosis was detected during laparoscopy. The woman had a regular menstrual cycle (28 ± 5 days), BMI 26 kg/m^2 and used no hormonal medications during the previous 3 months before laparoscopy. The endometrial biopsy samples were collected during the laparoscopy using an endometrial suction Pipelle catheter (Laboratoire CCD, France).

Processing of biopsies

The endometrial tissue biopsies for whole tissue study were placed into RNAlater (Ambion Inc., Austin, TX, USA) solution and stored at –80°C for further analysis. For cell-type-specific analysis, the endometrial tissue samples were placed immediately into the cryopreservation medium containing 1 × Dulbecco's Modified Eagle's Medium (DMEM) (Life Technologies, Carlsbad, CA, USA), 30% (v/v) fetal bovine serum (FBS) (Biowest, Riverside, MO, USA), and 7.5% (v/v) Dimethyl Sulfoxide Hybri-Max (Sigma, Ronkonkoma, NY, USA). The cryovials were put into a Nalgene Cryo 1°C 'Mr. Frosty' Freezing Container (Thermo Scientific, Waltham MA, USA) and placed into –80°C freezer overnight. The biopsies were stored in liquid nitrogen until use. Total RNA from whole tissue was extracted by using miRNeasy Mini kit following the manufacturer's protocol (Qiagen, Hilden, Germany). Handling, dissociation and preparation of endometrial biopsies for fluorescence-activated cell sorting (FACS) has been described in detail (*Krjutškov et al., 2016*). Briefly, the biopsied tissue samples were thawed, dissociated, and endometrial cells were stained with fluorochrome-conjugated antibodies (*Imai et al., 1992; Kato et al., 2007*). Stromal cells were stained with mouse anti-human CD13 monoclonal antibody (clone TUK1, R-Phycoerythrin) (Invitrogen, Waltham, MA, USA), epithelial cells were stained simultaneously with the fluorochrome-conjugated mouse anti-human CD9 monoclonal antibody (clone MEM-61, FITC) (Novus Biologicals, Centennial, CO, USA) and all dead cells were stained with DAPI (Invitrogen, USA). CD9 or CD13 positive and DAPI negative (alive) cells were sorted directly into QIAzol Lysis Reagent (Qiagen, Germany). Total RNA was isolated immediately using RNeasy Micro kit (Qiagen, Germany). The paired samples of (LH+2) and (LH+8) endometrial tissue biopsies from six healthy volunteers were used in immunohistochemistry. Tissue samples for histological assessment and immunohistochemical analysis were fixed and stored in 10% formalin solution. All samples used in our study, including two separate biopsies for Western blot analysis, are shown on the simplified menstrual cycle scheme (FIGURE 1).

Transcriptome data analysis

Two of our previously published RNA sequencing (RNA-seq) datasets were used to determine the expression of mucins in the whole endometrium and in sorted epithelial and stromal LH+2 and LH+8 endometrial cells (*Altmäe et al., 2017*). Both datasets are accessible via Gene Expression Omnibus (www.ncbi.nlm.nih.gov/geo/) under accession numbers GSE98386 and GSE97929, respectively. The paired-end 100 bp sequencing on Illumina HiSeq2500 instrument was used for transcriptome profiling for whole tissue samples (GSE98386) for 10 women, as described in our previous study (*Altmäe et al., 2017*). The cell-type-specific RNA-seq analysis was conducted with sorted epithelial and stromal cells (GSE97929) for 26 women, as also described in the same study (*Altmäe et al., 2017*), following our single-cell tagged reverse transcription (STRT) protocol (*Krjutškov et al., 2016*) with modifications for bulk RNA. In data analysis, STRTprep pipeline (v3dev branch, available at https://github.com/shka/STRTprep) was used for pre-processing and differential transcriptome expression analyses. This pipeline uses the SAMstrt package (*Katayama et al., 2013*), which includes the variation of SAM (significance analysis of microarrays) statistical test, adjusted to RNA-seq data (*Li and Tibshirani, 2011*). As this is a non-parametrical statistical test, this is more robust to outliers and to the deviations from the assumptions of parametrical methods (*Li and Tibshirani, 2011*).

Quantitative reverse transcription polymerase chain reaction

The *MUC1* and *MUC20* expression levels in whole endometrial biopsies were determined in 10 paired LH+2 and LH+8 endometrial samples. Cell-type-specific expression pattern was determined in 17 out of the 26 paired (LH+2 and LH+8) endometrial epithelial and stromal cell samples isolated by FACS method described previously (*Krjutškov et al., 2016*). DNase treated (TURBO DNA-free™ kit, Ambion Inc., USA) RNA was converted into cDNA using RevertAid First Strand cDNA Synthesis Kit (Thermo-Fisher Scientific Inc., Bartlesville, OK, USA). In accordance to conditions specified by the manufacturer, quantitative reverse transcription polymerase chain reaction (qRT-PCR) was conducted using 1 × HOT FIREPol EvaGreen qPCR Mix Plus (Solis BioDyne, Tartu, Estonia). The following primers were used: *MUC1* (Rev-TACCTGCAGAAACCTTCTCATAGG, Fw- CATCTTTCCAGCCCGGGATAC) and *MUC20* (Rev- CACGCAGTAAG GA GACCTGG, Fw- CGTGAGTGCAG GTGAAAATGG). The succinate dehydrogenase complex subunit A (*SDHA*: Rev- CCACCACTGCATCAAATTCATG, Fw- TGGGAACAAGAGGGCATCTG) was used as endogenous control. The expression differences between LH+2 and LH+8 were calculated using Welch two-sample t-test, and a *P*-value cut-off of $P < 0.05$. The $2^{-\Delta\Delta Ct}$ method was used for calculating the relative expression and the fold change between LH+2 and LH+8 samples (*Livak and Schmittgen, 2001*).

RNA interference-mediated knock-down of MUC20

Three unique 27mer small interfering RNA (siRNA) duplexes specific to human MUC20 and scrambled control siRNA (OriGene, Rockville, MD, USA) were transfected into epidermoid carcinoma cell line (A431) by using HiPerFect transfection reagent (Qiagen, Germany). A431 cell line was obtained from the American Type Culture Collection (ATCC). Transfection complexes were formed according to the manufacturer's instructions. On the day of transfection (0 h), 75.000 cells were seeded into each well of 24-well cell culture plate in 500 µl Iscove's modified Dulbecco's medium (IMDM medium) (Lonza, Basel, Switzerland) containing 10% (v/v) fetal bovine serum (FBS), (PAN Biotech, Aidenbach, Germany) and antibiotics mix suitable for cell culture (Penicillin (100 U/ml)/ Streptomycin (0.1 mg/ml), Naxo, Tartu, Estonia). Immediately after seeding, freshly formed transfection complexes were added drop-wise to the cells. The final concentration of siRNA was 7.5 nM. The next day (24 h), the culture medium

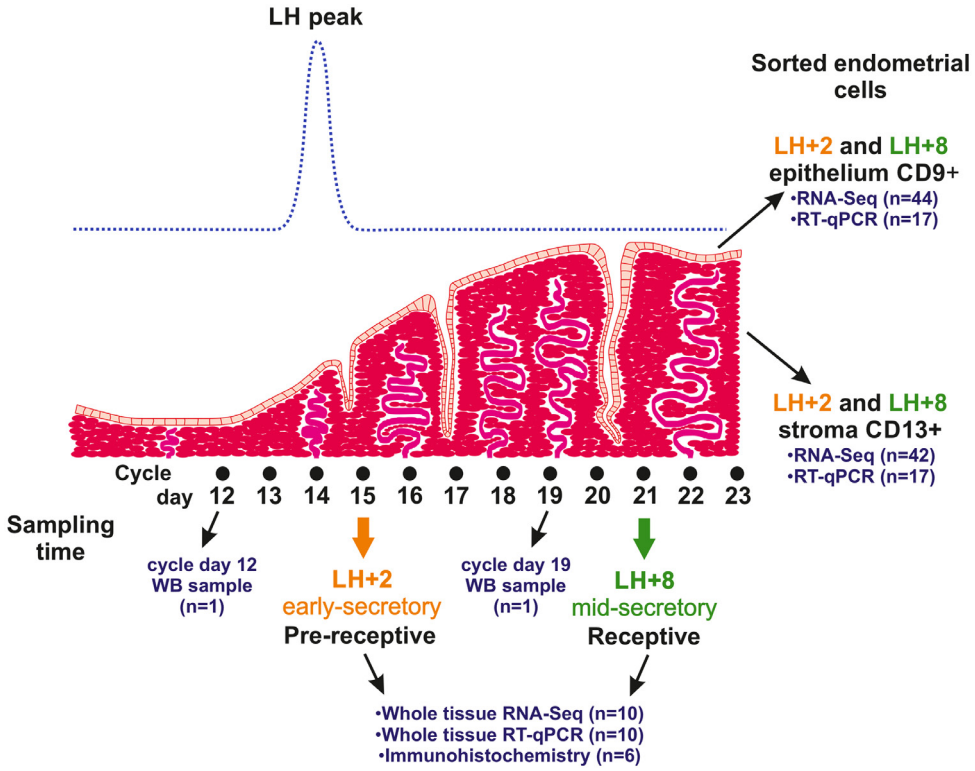

FIGURE 1 Different phases of the menstrual cycle showing the days when samples were collected in this study. Endometrial biopsies were obtained on day 2 and 8 after the LH surge (LH+2 and LH+8) during the same cycle. Paired samples (LH+2 and LH+8) from 10 women were used for whole tissue analyses and samples from 26 different women were used for endometrial epithelial and stromal cells analysis. Of the possible 104 samples from 26 women, the numbers suitable for RNA-sequencing (RNA-seq) and further validation were 18 for LH+2 epithelium, 26 for LH+8 epithelium, 20 for LH+2 stroma and 22 for LH+8 stroma. For samples from sorted cells, CD9 was considered as an epithelial marker and CD13 as a stromal marker. Two separate biopsies were obtained on cycle day 12 and cycle day 19 for primary cell culture and further protein analysis. The number of samples analysed on indicated days is shown in brackets (n). qRT-PCR, quantitative reverse transcription polymerase chain reaction; WB, Western blot.

was changed with fresh medium without complexes. Subsequently (48 h), cells were passaged 1:2 and transfected for the second time with the same protocol that was used for the first transfection. Next day (72 h), cells were lysed in radioimmunoprecipitation assay (RIPA) buffer containing 10 mM Tris-HCl (pH 7.2), 150 mM NaCl, 0.1% (w/v) sodium dodecyl sulfate (SDS), 1% (v/v) Triton X-100, 1% (w/v) sodium deoxycholate, 5 mM ethylenediaminetetraacetic acid (EDTA) and Complete protease inhibitor cocktail (Roche Diagnostics, Rotkreuz ZG, Switzerland) and stored at –80°C.

Cell culture

For isolation of primary cultures, the cryopreserved endometrial biopsy samples were thawed and washed twice with DMEM medium (Life Technologies, USA). The isolation and culturing of endometrial primary stromal and epithelial cells were carried out as described previously by *Chen and Roan (2015)* with minor modifications. In our protocol, the primary endometrial epithelial cells were plated on fibronectin-coated flasks (20 µg/2 ml/25 cm^2) (Sigma–Aldrich, St Louis, MO, USA) and trypsin-based detaching method was used for both, stromal and epithelial cells. The first passage of primary epithelial cells and the second passage of stromal cells were used for protein isolation. MCF-7 cell line, a human breast cancer cell line, was obtained from ATCC and cultured in DMEM (DMEM-11A, Capricorn Scientific, Ebsdorfergrund, Germany) with 10% (v/v) FBS (PAN Biotech, Germany) and cell culture antibiotics (Penicillin (100 U/ml)/ Streptomycin (0.1 mg/ml), Naxo, Estonia). MCF-7 cell line lysate was used as a negative control for MUC20 protein expression in Western blot experiments. The A431 cell line was obtained from ATCC and cultured in IMDM (Lonza, Switzerland) with 10% (v/v) FBS (PAN Biotech, Germany) and antibiotics (Penicillin (100 U/ml)/Streptomycin (0.1 mg/ml), Naxo, Estonia). Cell lines were cultured in the presence of 5% CO_2 at 37°C in humid conditions and passaged with 0.25% Trypsin-EDTA (Naxo, Estonia). Cells were lysed in RIPA buffer containing 10 mM Tris-HCl (pH 7.2), 150 mM NaCl, 0.1% (w/v) SDS, 1% (v/v) Triton X-100, 1% (w/v) sodium deoxycholate, 5 mM EDTA and Complete Protease Inhibitor Cocktail (Roche Diagnostics, Switzerland) and stored at –80°C.

SDS-PAGE and Western blotting

The protein concentration of samples in RIPA were measured with BCA Protein Assay Kit (Thermo Fisher Scientific, USA), and equal protein amounts for each sample were loaded onto 4–10% gradient SDS-PAGE gels for electrophoresis (Mini-Protean system) (Bio-Rad Laboratories, Philadelphia, PA, USA). The material was transferred to polyvinylidene difluoride membrane with Mini Trans-Blot Cell system (Bio-Rad Laboratories, USA). The membrane was washed with 1 × Tris-buffered saline + 0.1% (v/v) Tween 20 (TBS-T) and blocked with 2% (w/v) bovine serum albumin (Capricorn Scientific, Germany) dissolved in TBS-T (blocking solution) for 1 h followed by incubation with primary anti-MUC20 antibody (0.5 µg/ml, ab73043) (Abcam,

Cambridge, UK) in blocking solution overnight at 4°C. After washing with TBS-T, additional blocking with 2% (v/v) normal goat serum in TBS-T was carried out for 30 min. The membrane was then incubated with the respective secondary goat antibody (Santa-Cruz Biotechnology Inc., Santa Cruz, CA, USA) conjugated with horseradish peroxidase (HRP) for 1 h at room temperature. Finally, the membrane was rinsed three times with TBS-T for 15 min followed by incubation with Immobilon Western Chemiluminescent HRP Substrate solution (Millipore Corporation, Billerica, MA, USA). Chemiluminescent signal was detected with BioSpectrum 510 Imaging System with VisionWorks LS software (both UVP, LLC, USA).

Immunohistochemistry

For immunohistochemical (IHC) experiments, 4-µm sections from paraffin-embedded tissue blocks were mounted on Superfrost Plus (Thermo Scientific, USA) slides. Tissue sections on slides were deparaffinized and rehydrated according to standard protocol (Abcam IHC guide). Subsequently, sections were subjected to the antigen retrieval procedure. For antigen retrieval, slides were heated at 60°C for 16 h in 10 mM Na-citrate buffer (pH 6.0) with 0.05% (v/v) Tween 20 (Naxo, Estonia). After antigen retrieval, slides were cooled down to room temperature and washed with tap water for 10 min. All washing steps included 1 × Tris-buffered saline (TBS) with 0.025% (v/v) Triton X-100 (PanReac AppliChem, Darmstadt, Germany) as a washing buffer. For the immunohistochemistry procedure, a mouse and rabbit specific HRP/DAB (ABC) detection kit (ab64264) (Abcam, UK) was used. All steps were carried out according to the producer's protocol with only a few modifications. After protein blocking and washing steps, additional blocking against possible tissue endogenous biotin was applied, using endogenous avidin-biotin blocking system (ab3387) (Abcam, UK). Mouse polyclonal antibodies at concentration 5 µg/ml, obtained by immunization against the full-length protein (ab73043) (Abcam, UK), were used as primary anti-MUC20 antibodies in immunohistochemistry. Mouse immunoblobulin IgG_1 (MAB002), IgG_{2A} (MAB003), IgG_{2B} (MAB0041), and IgG_3 (MAB007) subclasses (all from R&D Systems, Minneapolis, MN, USA) were mixed and used for isotype control at the same concentrations as the primary antibody. Incubation with primary antibody and mouse non-specific IgG subclasses was carried out overnight in a humidity chamber at 4°C. For antibody dilution and incubation 1 × TBS buffer with 1% (w/v) bovine serum albumin (Capricorn Scientific, Germany) was used. After incubation with the primary antibody, an additional blocking step with 4% (v/v) normal goat serum (Abcam, UK) diluted in 1 × TBS buffer was carried out. Further steps were carried out as per manufacturer's protocol. Chromogenic reaction was developed for 6 min and stopped thereafter. Cell nuclei were counterstained with Mayer's haematoxylin solution for 1 min, and slides were then washed for 10 min with tap water. Slides were dehydrated through 30 s incubation in different ethanol and xylene solutions in opposite order of the rehydration step. Cover glasses were mounted with Eukitt (Sigma-Aldrich, USA) quick-hardening medium. Slides were investigated under an Olympus BX41 microscope with 10 ×, and 40 × magnification objectives and tissue microphotos were taken with an Olympus DP71 camera and Cell B (Olympus, Japan) software. Semi-quantitative analysis of IHC (n = 6) was conducted with ImageJ package Fiji version 1.52e (*Schindelin et al., 2012*). DAB signal intensity was measured separately for epithelial and stromal components of the endometrium. The relative DAB intensity was calculated according to the formula: f = 255-i, where 'f' is relative DAB intensity and 'i' is mean DAB intensity obtained from the software; 'i' ranges from 0 (zero – deep brown, highest expression), and 255 (total white). The method we used for the signal intensity measurements with ImageJ has been previously described for endometrial histological evaluation and consists of 10 image analysis steps that are precisely described in following publication (*Fuhrich et al., 2013*).

Statistical analysis

Mann–Whitney U test or Welch two-sample t-test was used to assess gene expression for significant differences between the pre-receptive (LH+2) and receptive (LH+8) phases using RNA-seq or qRT-PCR data, respectively. For correlation analysis, the changes in the *MUC20* gene expression (log_2 [fold-change] between LH+2 and LH+8) were compared with the changes in expression of other epithelial cells' genes. For that purpose, Spearman correlation test was used (Bonferroni corrected $P < 0.05$, $R > 0.8$). The enrichment of receptivity biomarkers in the human genome or in the *MUC20*-correlated gene subset was compared using Fisher's exact test. Statistical analyses and graphs were made in R (version 3.5.0). For semi-quantitative IHC analysis, DAB signal intensities were compared using paired t-test with a statistically significant P-value cut-off of $P < 0.05$. Statistical analysis and graph were prepared in Microsoft Office Excel (365 ProPlus, version 1809).

RESULTS

Endometrial epithelial cells express higher level of *MUC20* mRNA in the receptive than in the pre-receptive endometrium

To determine the repertoire of mucins that are expressed in different cell compartments of the human endometrium, two of our previously published RNA-seq datasets (GSE97929 and GSE98386) and profiled transcriptome expression were used either separately in stromal and epithelial cells (GSE97929), or in the whole endometrial tissue (GSE98386) during the pre-receptive (LH+2) and receptive (LH+8) phases (*Altmäe et al., 2017*). Cell-type specific RNA sequencing data (GSE97929) revealed the expression of eight different mucin mRNAs: *MUC1, MUC6, MUC13, MUC15, MUC20* and *MUC22* in stromal cells, and *MUC1, MUC4, MUC7, MUC13, MUC15, MUC20* and *MUC22* in epithelial cells (TABLE 1). *MUC6* and *MUC7* were only detected in one stromal or one epithelial sample, respectively. Most detected mucins were expressed only in 1-8 out of 18 analysed LH+2 stage or 1-14 out of 26 analysed LH+8 epithelial cell samples. *MUC1* was expressed in most of the epithelial samples analysed irrespective of the day (15/18 at LH+2; 24/26 at LH+8). In contrast, although *MUC20* was expressed only in five out of 18 epithelial samples on day LH+2, most samples (23/26) became positive for *MUC20* expression on day LH+8. Therefore, unlike *MUC1*, *MUC20* displayed a remarkable change in expression between the pre-receptive and receptive phases. Next, the expression levels of *MUC1* and *MUC20* were studied further in the analysed cell-specific samples and provided as RNA-seq normalized read counts in Supplementary Table 1. *MUC1* expression was similar between the LH+2 and LH+8 endometria, both within the epithelial and stromal cell populations (FIGURE 2). When *MUC1* expression was compared

TABLE 1 EXPRESSION OF DIFFERENT MUCIN mRNAs IN HUMAN ENDOMETRIAL EPITHELIAL AND STROMAL CELLS

	MUC1, n (%)	*MUC4*, n (%)	*MUC6*, n (%)	*MUC7*, n (%)	*MUC13*, n (%)	*MUC15*, n (%)	*MUC20*, n (%)	*MUC22*, n (%)
Epithelium LH + 2	15/18 (83.3)	1/18 (5.6)	0/18 (0)	0/18 (0)	4/18 (22.2)	8/18 (44.4)	5/18 (27.8)	3/18 (16.7)
Epithelium LH + 8	24/26 (92.3)	3/26 (11.5)	0/26 (0)	1/26 (3.8)	14/26 (53.8)	11/26 (42.3)	23/26 (88.5)	1/26 (3.8)
Stroma LH + 2	9/20 (45)	0/20 (0)	1/20 (5)	0/20 (0)	1/20 (5)	3/20 (15)	2/20 (10)	4/20 (20)
Stroma LH + 8	12/22 (54.5)	0/22 (0)	0/22 (0)	0/22 (0)	1/22 (4.5)	4/22 (18.2)	10/22 (45.5)	2/22 (9.1)

Data are based on the published cell-type specific RNA-sequencing (GSE97929) (*Altmäe et al., 2017*). For each tissue sample, the ratio of positive samples (detected/analysed) and the percentage of positive samples that express the indicated mucin (in parenthesis) are shown.

between epithelial and stromal cells in LH+2 and LH+8 phases, it seemed that *MUC1* expression was significantly higher in epithelial cells irrespective of the cycle day ($P = 0.005$ at LH+2 and $P = 0.006$ at LH+8). In contrast, the expression of *MUC20* was significantly higher in the LH+8 cycle phase compared with LH+2 in the epithelial cells ($P = 0.005$). Since *MUC20* expression was detected only in two samples out of 20 in early secretory (LH+2) stromal cells (TABLE 1), no comparison betwen *MUC20* expression and different phases in stromal cells could be made. Further, the expression level of *MUC1* and *MUC20* was compared in the whole endometrium RNA-seq dataset (GSE98386). In the whole endometrial tissue ($n = 10$), *MUC1* expression was not statistically different between the LH+2 and LH+8, whereas *MUC20* expression was significantly higher in the receptive LH+8 endometrium ($P = 7.58 \times 10^{-5}$, Mann–Whitney' test). *MUC1* and *MUC20* normalized read counts in whole tissue samples are given in Supplementary Table 1.

The expression of *MUC1* and *MUC20* was validated by qRT-PCR in the whole tissue and in the sorted endometrial epithelial and stromal cells (FIGURE 3). Our results corresponded well with RNA-seq data, showing that *MUC1* expression was significantly higher in epithelial cells compared with stromal cells in both cycle phases ($P = 3.4 \times 10^{-4}$ at LH+2; $P = 0.006$ at LH+8). Importantly, qRT-PCR analysis confirmed that *MUC20* expression differed between LH+2 and LH+8 phases in the whole endometrium ($P = 1.1 \times 10^{-4}$) and in epithelial cells ($P = 0.039$). Again, *MUC20* expression was not significantly different between different cycle days in stromal cells. We also noticed that *MUC20* expression was remarkably higher in epithelial cells than in stromal cells specifically in the receptive (LH+8) phase ($P = 0.002$). Taken together, our results demonstrate that the *MUC20* transcription is increased in epithelial cells during the transition from the pre-receptive to the receptive phase.

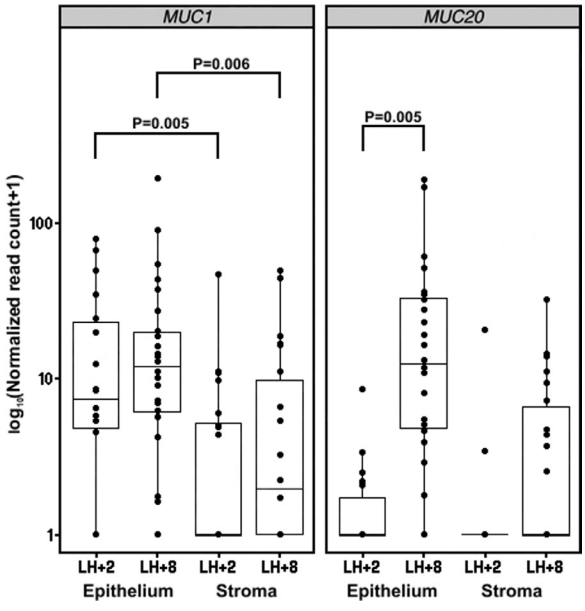

FIGURE 2 The levels of *MUC1* and *MUC20* mRNAs in sorted human endometrial cells based on our published RNA-seqencing dataset (GSE97929) (*Altmäe et al., 2017*). Early secretory (LH+2) and mid-secretory (LH+8) endometrial epithelial ($n = 44$) and stromal ($n = 42$) cells were analysed. The Mann–Whitney U test was used to compare the gene expression changes between the samples. Results are presented as a boxplot diagram where median values are marked as black lines inside boxes, which show interquartile range.

MUC20 protein is expressed predominantly in endometrial epithelial cells

Next, we aimed to confirm whether the expression of MUC20 seen at the mRNA level in epithelial and stromal cells is the same at the protein level. MUC20 protein expression was analysed by Western blot in cultured primary epithelial and stromal cells. Both cell types were isolated from two endometrial biopsies. One was collected on menstrual cycle day 12, which corresponds to the end of the proliferative phase (close to LH+2) and the other on menstrual cycle day 19, which corresponds to the beginning of the mid-secretory phase (close to LH+8) (FIGURE 1). An anti-MUC20 antibody was used, which was validated in epidermoid carcinoma cell line A431 that is known to express MUC20, by using RNAi-mediated silencing of MUC20 (FIGURE 4A). A431 cells were transfected with three different siRNAs against *MUC20* in parallel with a scrambled control siRNA and detected MUC20 expression by Western blot analysis. A notable decrease in the expression of MUC20 at 95-130 kDa in A431 cells with all siRNAs was observed, strongly suggesting that the anti-MUC20 antibody used specifically recognises MUC20. Next, MUC20 expression was detected separately in cultured endometrium-derived epithelial and stromal cells using A431 cells as a positive and breast adenocarcinoma cell line

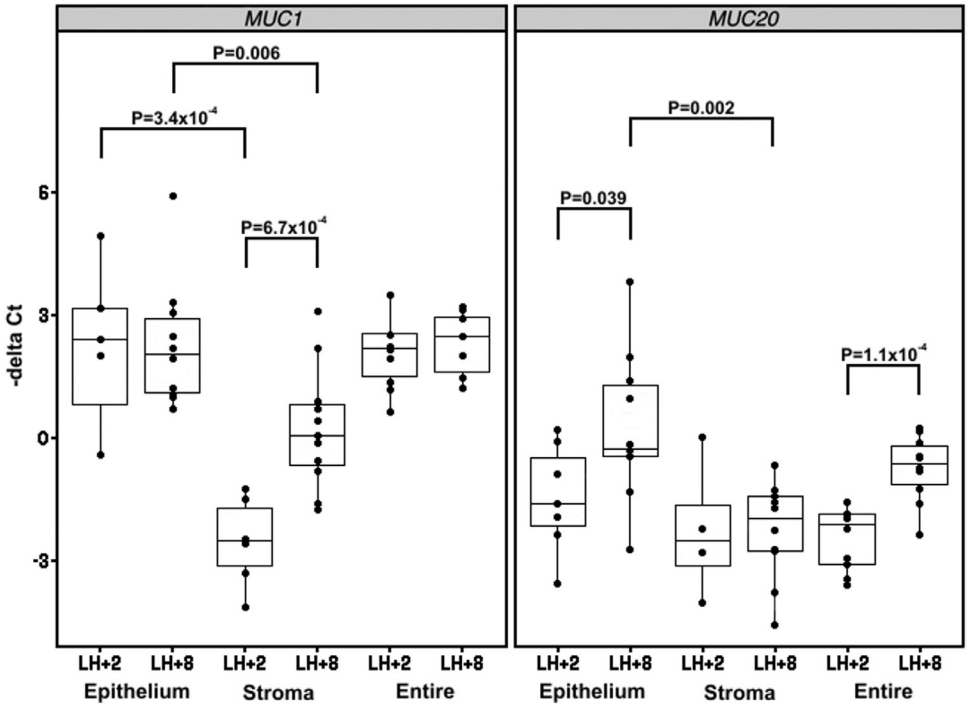

FIGURE 3 The levels of *MUC1* and *MUC20* mRNAs were validated by reverse transcription quantitative polymerase chain reaction. Early secretory (LH+2) and mid-secretory (LH+8) endometrial epithelial (n = 17) and stromal (n = 17) cells or whole endometrial tissue samples (n = 10) were analysed. The gene expression changes were subjected to Welch two-sample t-test. Results are presented as a boxplot diagram; median values are marked as black lines inside boxes, which show interquartile range.

MCF-7 as a negative control (FIGURE 4B). MUC20 protein was expressed at a much higher level in the epithelial cells compared with stromal cells derived from both biopsies (cycle day 12 and 19). MUC20 expression in epithelial cells cultured from cycle day 12 biopsy seems to be weaker than from cycle day 19. Only one sample was available from cycle day 12 (close to LH+2) and one sample from cycle day 19 (close to LH+8); this was, therefore, insufficient for statistical analysis. From these two biopsies, however, we observed that cycle phase-independent MUC20 protein expression was higher in the epithelial cells (FIGURE 4B). The nearly undetectable expression of MUC20 in stromal cells in Western blot analysis also coincided well with the low level of its transcript in stromal cells irrespective of the cycle day (FIGURE 2 and FIGURE 3). Therefore, we conclude that the epithelial cells are the major source of MUC20 protein in the endometrium.

Immunohistological detection of MUC20 localization in the endometrium in the pre-receptive and receptive phases

Next, we set out to determine the localization of MUC20 expression in the intact endometrial tissue using IHC. The endometrial tissue was isolated from six healthy women both at cycle days LH+2 and LH+8. Only slight, almost undetectable MUC20 expression was detected in the endometrial tissue sections in the pre-receptive phase (FIGURE 5A, FIGURE 5C and FIGURE 5E), which was remarkably increased in the receptive phase. The expression of MUC20 was stronger, particularly in the glandular and luminal epithelial cell compartments (FIGURE 5B, FIGURE 5D and FIGURE 5F), and less so in the stromal compartment at LH+8. The semi-quantitative analysis confirmed that MUC20 expression is increased at the LH+8 stage compared with the LH+2 in the endometrial epithelial cells (n = 6, P = 0.029), whereas stromal MUC20 expression was similar between these two stages (FIGURE 5I). These results confirm that MUC20 expression is markedly higher in the receptive than in the pre-receptive endometrial epithelium.

MUC20 expression is correlated with other receptivity biomarkers

To identify the genes that change expression together with MUC20 in the epithelial cells between the pre-receptive (LH+2) and receptive phases (LH+8), the transcriptome expression of the epithelial cells from our previous cell-specific RNA-seq dataset (GSE97929) was analysed (*Altmäe et al., 2017*). A total of 386 genes whose expression was highly correlated with *MUC20* was found (Spearman correlation test; Bonferroni corrected $P < 0.05$, $R > 0.8$) (Supplementary Table 2). Importantly, several previously known endometrial–epithelial receptivity marker genes including *DPP4*, *TSPAN8*, *CP*, *COMP*, *LAMB3*, *ANXA4* and *ARID5B* were found among the differentially expressed genes (Supplementary Table 2). Moreover, receptivity biomarkers were 7.98 times over-represented among *MUC20*-correlated genes compared with the rest of the protein-coding genes in the human genome (Fisher's exact test, two-sided $P = 6.47 \times 10^{-5}$). This finding verifies the receptive phase-specific expression of MUC20 in the human endometrium.

A model of MUC20 interaction with the mesenchymal–epithelial transition receptor in the receptive endometrium

Mesenchymal–epithelial transition (MET) receptor mediates stromal cell-secreted hepatocyte growth factor (HGF)-signalling that is important for epithelial proliferation and survival (*Bottaro et al., 1991; Montesano et al., 1991; Rubin et al., 1991*). It has been shown that MUC20 can interact with the

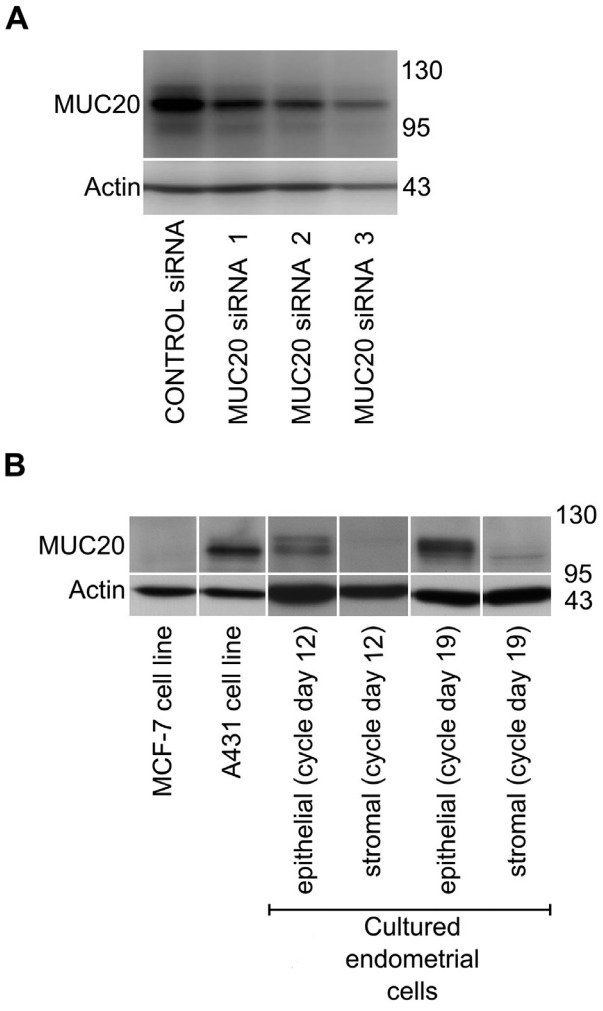

FIGURE 4 MUC20 protein is expressed in human endometrium. (A) Validation of an anti-MUC20 antibody in A431 cell line with three different small interfering (si)RNAs against MUC20; (B) the expression of MUC20 in primary cultured endometrial epithelial (n = 2) and stromal (n = 2) cells. Cells isolated from cycle day 12 and 19 biopsies. The A431 cell line was used as a positive and MCF-7 cell line as a negative control. The expression of actin was used as a loading control. Molecular weight markers are given in kilodaltons on the right hand side.

cytoplasmic tail of the MET receptor that results in the suppression of epithelial proliferation (*Higuchi et al., 2004a*). Therefore, a decision was made to use cell-type-specific RNA sequencing data (GSE97929) to investigate changes in *MET* expression between the pre-receptive LH+2 and receptive LH+8 endometrium. *MET* expression was found to be highly correlated with the *MUC20* expression in endometrial epithelial cells (Spearman correlation test; Bonferroni corrected P = 0.000994, R = 0.898) (Supplementary Table 2). Moreover, expression of both HGF mRNA in stromal cells and MET mRNA in epithelial cells increased during the transition between the pre-receptive and receptive phases (FIGURE 6). Such synchronous changes in the expression of MUC20 and MET in the epithelium and HGF in the stroma between the LH+2 and LH+8 phases raises the possibility that MUC20 could function in blocking MET-mediated signalling pathway during the WOI.

DISCUSSION

Our study has identified increased MUC20 expression in the receptive endometrium epithelium, and we propose it as a new promising biomarker candidate of endometrial receptivity that needs to be validated further to prove its ability to define the WOI. High expression of *MUC1* already in the pre-receptive phase has been previously reported (*Aplin et al., 2001*). Our results coincide with an earlier study, which detected *MUC1* expression both in the pre-receptive and receptive phases, thus not allowing us to distinguish between different cycle days based on *MUC1* expression (*Jeschke et al., 2009*).

MUC20 mRNA expression has previously been documented in the endometrial tissue using microarray-based gene expression analysis (*Evans et al., 2012*). Information about MUC20 protein expression in the human endometrium, however, is completely lacking. Here, we provide clear evidence that, unlike *MUC1, MUC20* expression is dynamically regulated during the menstrual cycle. We detected a significant increase in *MUC20* expression during the transition from the pre-receptive to the receptive phase of the endometrium. This change also occurred at the protein level, and more importantly, differential expression of MUC20 protein was specifically detected in the endometrial epithelium. Strikingly, *MUC20* expression was correlated well with other epithelial receptivity markers. The previously defined receptivity biomarkers (*Altmäe et al., 2017*) were almost eight times over-represented among *MUC20* correlated genes against the whole human genome. MUC20 expression correlation with previously known receptivity markers does not automatically mean that MUC20 itself plays an important role in the receptivity process, to reveal that, further clinical validation and functional studies are crucial. MUC20 coexpression with other endometrial receptivity markers, however, verifies that MUC20 expression is receptive phase-specific in human endometrium. Therefore, this knowledge is essential if we think about more precise dating of the implantation window. From an endometrial dating perspective, it is crucial that MUC20 expression is increased in the receptive endometrium, but if we want to compare it with currently used markers, larger cohorts of patients need to be analysed in the clinical validation studies. Some limitations of our study, however, should also be highlighted. In our study, we showed that both epithelial MUC20 mRNA and protein levels change when the endometrial tissue becomes receptive. As post-receptive endometrial samples were not available for this study, it is impossible to say whether the MUC20 expression declines or remains at the same level until the onset of menstruation. We are unable to provide data on whether the receptivity marker MUC20 may be altered in different patient groups, where

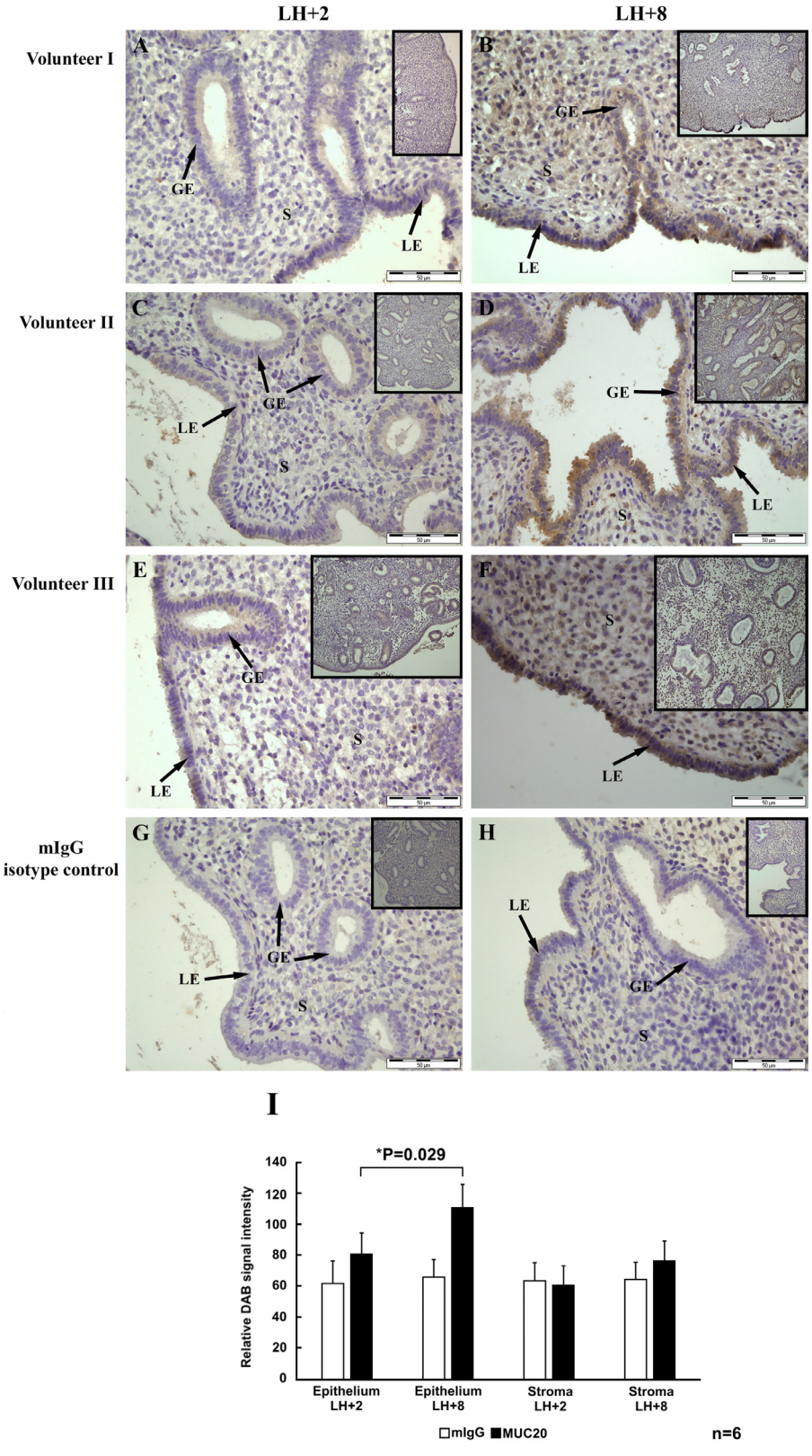

FIGURE 5 MUC20 protein expression and localization in the endometrial tissue in early secretory (LH+2) and mid-secretory (LH+8) endometrium visualized using immunohistochemistry (n = 6). Tissue samples of six fertile volunteers were analysed in early secretory and mid-secretory phases of the menstrual cycle. Representative images of the MUC20 expression in the three tissue samples in early-secretory (A, C, E) and mid-secretory (B, D, F) phases of the menstrual cycle. Mouse immunoglobulin was used as an isotype control for both phases (G, H). The ground images of the tissue contain 50-µm scale bars, and lower magnification images bordered by black line are one-fourth magnification of the ground images. Semi-quantification of all immunohistochemistry (n = 6) results (I). Relative DAB signal intensity was measured with ImageJ package Fiji and paired t-test was used to compare results (values are mean ±SD). GE, glandular epithelium; LE, luminal epithelium; S, stroma.

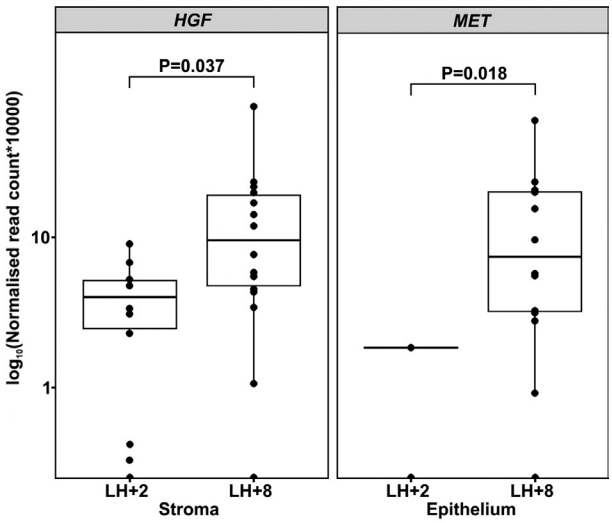

FIGURE 6 The levels of hepatocyte growth factor (*HGF*) and mesenchymal–epithelial transition receptor (*MET*) mRNAs in endometrial stromal and epithelial cells, respectively, based on our published RNA-sequencing data (*Altmäe et al., 2017*). Early secretory (LH+2) and mid-secretory (LH+8) endometrial stromal (n = 42) and epithelial (n = 44) cells were analysed. The Mann–Whitney U test was used to compare the gene expression changes between the samples. Results are presented as a boxplot diagram where median values are marked as black lines inside boxes, which show interquartile range.

the endometrial receptivity is affected. Also, the benefit of MUC20 in clinical settings can only be confirmed if data concerning embryo transfer success is ascertained in an appropriately designed trial. Furthermore, we acknowledge that the sample size of our study is relatively low and we cannot entirely exclude the presence of undiagnosed asymptomatic endometriosis cases among the control women, which may theoretically bias the conclusions of the present study.

To date, the physiological function of MUC20, which is not related to cancer, has been described in kidney cells. It has been shown that MUC20 participates in the regulation of HGF-activated MET receptor-mediated pathway in the renal tubule epithelium (*Higuchi et al., 2004a*). Stromal cells resident in a wide variety of different tissues are producing HGF that is used by epithelial cells via MET receptor (*Bottaro et al., 1991; Montesano et al., 1991; Rubin et al., 1991*). We found that the expression of *MET* in the epithelium and *HGF* in the stroma increased in the receptive endometrium compared with the pre-receptive endometrium. Moreover, *MET* expression was highly correlated with *MUC20* expression in the epithelial cells. Consistently, the up-regulation of *MET* mRNA during the WOI has been previously observed by others (*Evans et al., 2012*).

Previously, it has been shown that MUC20 interaction with the MET receptor blocks a signalling cascade leading to the inhibition of cell proliferation (FIGURE 7A). This interaction, however, does not affect cell scattering, morphogenesis and cell survival (*Higuchi et al., 2004a*). We propose a similar function of MUC20 to be present in the human receptive endometrium at a time when the proliferation rate of the epithelial cells slows down (FIGURE 7B). Although this hypothesis is intriguing, we cannot provide any direct support for it, because it is difficult to establish the experimental model to prove this claim. It is well known that the endometrial primary epithelial cells are difficult to maintain in culture, and their passage is often limited to only single passage (*Kyo et al., 2003; Chen et al., 2016; Masuda et al., 2016*). As epithelial cells are highly differentiated, strongly self-adherent and have to be polarized to maintain apical and basolateral morphology, the culturing of these cells is much more difficult compared with their stromal

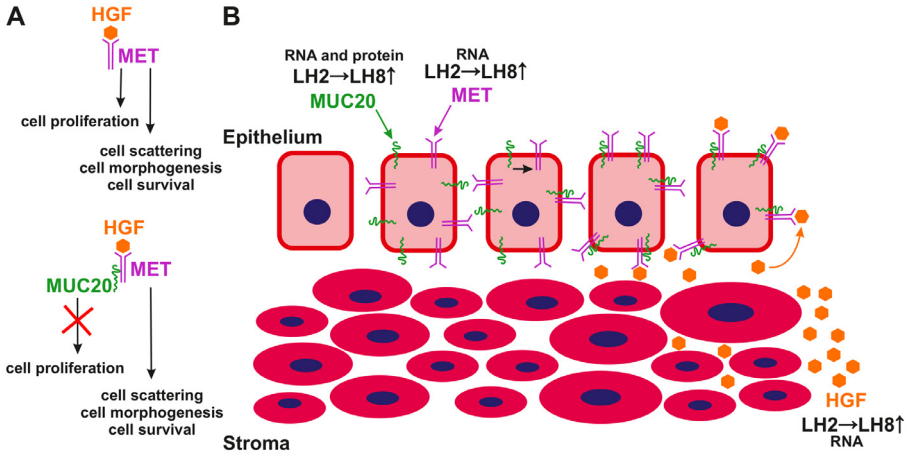

FIGURE 7 An interaction of MUC20 with the mesenchymal–epithelial transition (MET) receptor signalling. (A) The interaction of MUC20 with MET receptor blocks hepatocyte growth factor (HGF)-induced proliferation of epithelial cells, which was shown previously in the case of renal tubule epithelium (*Higuchi et al., 2004a*); (B) A hypothetical model of MUC20 interaction with the MET receptor in the human endometrium during window of implantation. The expression of MUC20 and MET increase in the epithelial cells at LH+8, with the concomitant increase of HGF expression in stromal cells. This regulation by MUC20 may prove to be important for the successful preparation of the endometrium for embryo implantation.

counterparts, mostly because of their limited expansion potential and extremely short life-span. This is the reason why we were unable to apply our MUC20 knock-down protocol in these demanding cells. Endometrial epithelial cell lines like Ishikawa, HEC-1A or RL95-2 are also not suitable as a model for studying the functions of MUC20 in endometrial receptivity because of their cancerous origin. In different types of cancers and particularly endometrial cancers mucins expression is aberrant and MUC20 is no exception from that, as overexpression of MUC20 in endometrial cancers is known to lead to the more malignant and aggressive phenotype (*Chen et al., 2013; Zheng et al., 2019*).

Because of the aforementioned difficulties in controlling our hypothesis in the endometrial model, we can only rely on a recent functional study on pancreatic ductal adenocarcinoma cells where MUC20 was silenced. Co-immunoprecipitation revealed the physical association of MUC20 and MET. Moreover, MUC20 silencing suppressed the MET- and HGF-induced malignant phenotype, e.g. high proliferation and viability, migration, invasion, of cancer cells (*Chen et al., 2018*). That coincides well with our hypothesis that MUC20 and MET also interact in human endometrium, but at the moment we only have indirect confirmation of our hypothesis, and we do not know exact mechanisms of that interaction due to difficulties in performing MUC20 knock-down or other functional studies using primary endometrial epithelial cells. Our model of potential interaction of MUC20 and MET in the receptive endometrium is also supported by an interactome study of human embryo implantation that speculated on the potential function of signalling networks within the endometrial tissue (*Altmäe et al., 2012*).

In conclusion, to our knowledge this is the first study to report the cycle-dependent expression of *MUC20* in the human endometrium at mRNA and protein levels. An implication of this study is the possibility that MUC20 could be included in the list of endometrial receptivity markers after further precise clinical validation. Maybe that will help us to better determine the endometrial receptivity status in the future. Further investigation, however, should also reveal the exact connection between MUC20 and HGF-activated MET receptor signalling in the human endometrium or disprove our hypothesis.

ACKNOWLEDGEMENTS

The authors would like to thank Külli Samuel from the Competence Centre on Health Technologies for the assistance with cell cultures and biopsy samples processing.

DECLARATION OF INTERESTS

This work was supported by the Estonian Ministry of Education and Research (grant no IUT34-16); by the Enterprise Estonia (grant no EU48695); by the EU FP7-PEOPLE-2012-IAPP project SARM (grant no EU324509); by the European Commission Horizon 2020 research and innovation programme under grant agreement 692065 (project WIDENLIFE); and MSCA-RISE-2015 project MOMENDO (grant no 691058). The authors report no financial or commercial conflicts of interest.

SUPPLEMENTARY MATERIALS

Supplementary material associated with this article can be found, in the online version, at doi:10.1016/j.rbmo.2019.05.004.

REFERENCES

Altmäe, S., Esteban, F.J., Stavreus-Evers, A., Simón, C., Giudice, L., Lessey, B.A., Horcajadas, J.A., Macklon, N.S., D'Hooghe, T., Campoy, C., Fauser, B.C., Salamonsen, L.A., Salumets, A. **Guidelines for the design, analysis and interpretation of "omics" data: Focus on human endometrium.** Hum. Reprod. Update 2014; 20: 12–28. https://doi.org/10.1093/humupd/dmt048

Altmäe, S., Koel, M., Võsa, U., Adler, P., Suhorutšenko, M., Laisk-Podar, T., Kukushkina, V., Saare, M., Velthut-Meikas, A., Krjutškov, K., Aghajanova, L., Lalitkumar, P.G., Gemzell-Danielsson, K., Giudice, L., Simón, C., Salumets, A. **Meta-signature of human endometrial receptivity: a meta-analysis and validation study of transcriptomic biomarkers.** Sci. Rep. 2017; 7: 10077. https://doi.org/10.1038/s41598-017-10098-3

Altmäe, S., Reimand, J., Hovatta, O., Zhang, P., Kere, J., Laisk, T., Saare, M., Peters, M., Vilo, J., Stavreus-Evers, A., Salumets, A. **Research Resource: Interactome of Human Embryo Implantation: Identification of Gene Expression Pathways, Regulation, and Integrated Regulatory Networks.** Mol. Endocrinol. 2012; 26: 203–217. https://doi.org/10.1210/me.2011-1196

Aplin, J.D., Meseguer, M., Simón, C., Ortíz, M.E., Croxatto, H., Jones, C.J. **MUC1, glycans and the cell-surface barrier to embryo implantation.** Biochem. Soc. Trans. 2001; 29: 153–156. https://doi.org/10.1042/0300-5127:0290153

Aplin, J.D., Seif, M.W., Graham, R.A., Hey, N.A., Behzad, F., Campbell, S. **The Endometrial Cell Surface and Implantation: Expression of the Polymorphic Mucin MUC–1 and Adhesion Molecules during the Endometrial Cycle.** Ann. N. Y. Acad. Sci. 1994; 734: 103–121. https://doi.org/10.1111/j.1749-6632.1994.tb21739.x

Bottaro, D.P., Rubin, J.S., Faletto, D.L., Chan, a M., Kmiecik, T.E., Vande Woude, G.F., Aaronson, S. a **Identification of the hepatocyte growth factor receptor as the c-met proto-oncogene product.** Science 1991; 251: 802–804. https://doi.org/10.1126/science.1846706

Carson, D.D., Lagow, E., Thathiah, A., Al-Shami, R., Farash-Carson, M.C., Vernon, M., Yuan, L., Fritz, M.A., Lessey, B. **Changes in gene expression during the early to mid-luteal (receptive phase) transition in human endometrium detected by high-density microarray screening.** Mol. Hum. Reprod. 2002; 8: 871–879. https://doi.org/10.1093/molehr/8.9.871

Chen, C.H., Wang, S.W., Chen, C.W., Huang, M.R., Hung, J.S., Huang, H.C., Lin, H.H., Chen, R.J., Shyu, M.K., Huang, M.C. **MUC20 overexpression predicts poor prognosis and enhances EGF-induced malignant phenotypes via activation of the EGFR-STAT3 pathway in endometrial cancer.** Gynecol. Oncol. 2013; 128: 560–567. https://doi.org/10.1016/j.ygyno.2012.12.012

Chen, J., Roan, N. **Isolation and Culture of Human Endometrial Epithelial Cells and Stromal Fibroblasts.** BIO-PROTOCOL 2015; 5. https://doi.org/10.21769/BioProtoc.1623

Chen, J.C., Hoffman, J.R., Arora, R., Perrone, L.A., Gonzalez-Gomez, C.J., Vo, K.C., Laird, D.J., Irwin, J.C., Giudice, L.C. **Cryopreservation and recovery of human endometrial epithelial cells with high viability, purity, and functional fidelity.** Fertil. Steril. 2016; 105: 501–510.e1. https://doi.org/10.1016/j.fertnstert.2015.10.011

Chen, S.T., Kuo, T.C., Liao, Y.Y., Lin, M.C., Tien, Y.W., Huang, M.C. **Silencing of MUC20 suppresses the malignant character of pancreatic ductal adenocarcinoma cells through inhibition of the HGF/MET pathway.** Oncogene 2018: 1–13. https://doi.org/10.1038/s41388-018-0403-0

Corfield, A. **Eukaryotic protein glycosylation: a primer for histochemists and cell biologists.** Histochem. Cell Biol. 2017; 147: 119–147. https://doi.org/10.1007/s00418-016-1526-4

Corfield, A.P. **Mucins: A biologically relevant glycan barrier in mucosal protection.** Biochim. Biophys. Acta - Gen. Subj. 2015; 1850: 236–252. https://doi.org/10.1016/j.bbagen.2014.05.003

Dharmaraj, N., Chapela, P.J., Morgado, M., Hawkins, S.M., Lessey, B.A., Young, S.L., Carson, D.D. **Expression of the transmembrane mucins, MUC1, MUC4 and MUC16, in normal endometrium and in endometriosis.** Hum. Reprod. 2014; 29: 1730–1738. https://doi.org/10.1093/humrep/deu146

Díaz-Gimeno, P., Horcajadas, J.A., Martinez-Conejero, J.A., Esteban, F.J., Alama, P., Pellicer, A., Simon, C. **A genomic diagnostic tool for human endometrial receptivity based on the transcriptomic signature.** Rev. Iberoam. Fertil. y Reprod. Humana 2011; 27: 337–351. https://doi.org/10.1016/j.fertnstert.2010.04.063

Enders, A.C., Hendrickx, A.G., Schlafke, S. **Implantation in the rhesus monkey: Initial penetration of endometrium.** Am. J. Anat. 1983; 167: 275–298. https://doi.org/10.1002/aja.1001670302

Evans, G.E., Phillipson, G.T.M., Sin, I.L., Frampton, C.M.A., Kirker, J.A., Bigby, S.M., Evans, J.J. **Gene expression confirms a potentially receptive endometrium identified by histology in fertile women.** Hum. Reprod. 2012; 27: 2747–2755. https://doi.org/10.1093/humrep/des233

Fuhrich, D.G., Lessey, B.A., Savaris, R.F. **Comparison of HSCORE Assessment of Endometrial β3 Integrin Subunit Expression with Digital HSCORE Using Computerized Image Analysis (ImageJ).** Anal Quant Cytopathol Histpathol 2013; 35: 210–216. https://doi.org/10.1021/nl061786n.Core-Shell

Germeyer, A., Savaris, R.F., Jauckus, J., Lessey, B. **Endometrial beta3 Integrin profile reflects endometrial receptivity defects in women with unexplained recurrent pregnancy loss.** Reprod. Biol. Endocrinol. 2014; 12: 53. https://doi.org/10.1186/1477-7827-12-53

Gipson, I.K., Blalock, T., Tisdale, A., Spurr-Michaud, S., Allcorn, S., Stavreus-Evers, A., Gemzell, K. **MUC16 Is Lost from the Uterodome (Pinopode) Surface of the Receptive Human Endometrium: In Vitro Evidence That MUC16 Is a Barrier to Trophoblast Adherence1.** Biol. Reprod. 2008; 78: 134–142. https://doi.org/10.1095/biolreprod.106.058347

Haouzi, D., Mahmoud, K., Fourar, M., Bendhaou, K., Dechaud, H., De Vos, J., Rème, T., Dewailly, D., Hamamah, S. **Identification of new biomarkers of human endometrial receptivity in the natural cycle.** Hum. Reprod. 2009; 24: 198–205. https://doi.org/10.1093/humrep/den360

Hattrup, C.L., Gendler, S.J. **Structure and Function of the Cell Surface (Tethered) Mucins.** Annu. Rev. Physiol. 2008; 70: 431–457. https://doi.org/10.1146/annurev.physiol.70.113006.100659

Hertig, A.T., Rock, J., Adams, E.C. **A description of 34 human ova within the first 17 days of development.** Am. J. Anat. 1956; 98: 435–493. https://doi.org/10.1002/aja.1000980306

Hey, N.A., Graham, R.A., Seif, M.W., Aplin, J.D. **The polymorphic epithelial mucin MUC1 in human endometrium is regulated with maximal expression in the implantation phase.** J. od Clin. Endocrinol. snd Metab. 1994: 337–342. https://doi.org/https://doi.org/10.1210/jcem.78.2.8106621

Higuchi, T., Orita, T., Katsuya, K., Yamasaki, Y., Akiyama, K., Li, H., Yamamoto, T., Saito, Y., Nakamura, M. **MUC20 suppresses the hepatocyte growth factor-induced Grb2-Ras pathway by binding to a multifunctional docking site of met.** Mol. Cell. Biol. 2004; 24: 7456–7468. https://doi.org/10.1128/MCB.24.17.7456-7468.2004

Higuchi, T., Orita, T., Nakanishi, S., Katsuya, K., Watanabe, H., Yamasaki, Y., Waga, I., Nanayama, T., Yamamoto, Y., Munger, W., Sun, H.W., Falk, R.J., Jennette, J.C., Alcorta, D.A., Li, H., Yamamoto, T., Saito, Y., Nakamura, M. **Molecular Cloning, Genomic Structure, and Expression Analysis of MUC20, a Novel Mucin Protein, Up-regulated in Injured Kidney.** J. Biol. Chem. 2004; 279: 1968–1979. https://doi.org/10.1074/jbc.M304558200

Hu, S., Yao, G., Wang, Y., Xu, H., Ji, X., He, Y., Zhu, Q., Chen, Z., Sun, Y. **Transcriptomic changes during the pre-receptive to receptive transition in human endometrium detected by RNA-Seq.** J. Clin. Endocrinol. Metab. 2014; 99: E2744–E2753. https://doi.org/10.1210/jc.2014-2155

Imai, K., Maeda, M., Fujiwara, H., Okamoto, N., Kariya, M., Emi, N., Takakura, K., Kanzaki, H., Mori, T. **Human endometrial stromal cells and decidual cells express cluster of differentiation (CD) 13 antigen/aminopeptidase N and CD10 antigen/neutral endopeptidase.** Biol. Reprod. 1992; 46: 328–334

Jeschke, U., Walzel, H., Mylonas, I., Papadopoulos, P., Shabani, N., Kuhn, C., Schulze, S., Friese, K., Karsten, U., Anz, D., Kupka, M.S. **The human endometrium expresses the glycoprotein mucin-1 and shows positive correlation for Thomsen-Friedenreich epitope expression and galectin-1 binding.** J. Histochem. Cytochem. 2009; 57: 871–881. https://doi.org/10.1369/jhc.2009.952085

Katayama, S., Töhönen, V., Linnarsson, S., Kere, J. **SAMstrt: Statistical test for differential expression in single-cell transcriptome with spike-in normalization.** Bioinformatics 2013; 29: 2943–2945. https://doi.org/10.1093/bioinformatics/btt511

Kato, K., Yoshimoto, M., Kato, K., Adachi, S., Yamayoshi, A., Arima, T., Asanoma, K., Kyo, S., Nakahata, T., Wake, N. **Characterization of side-population cells in human normal endometrium.** Hum. Reprod. 2007; 22: 1214–1223. https://doi.org/10.1093/humrep/del514

Koscinski, I., Viville, S., Porchet, N., Bernigaud, A., Escande, F., Defossez, A., Buisine, M.P. **MUC4 gene polymorphism and expression in women with implantation failure.** Hum. Reprod. 2006; 21: 2238–2245. https://doi.org/10.1093/humrep/del189

Krjutškov, K., Katayama, S., Saare, M., Vera-Rodriguez, M., Lubenets, D., Samuel, K., Laisk-Podar, T., Teder, H., Einarsdottir, E., Salumets, A., Kere, J. **Single-cell transcriptome analysis of endometrial tissue.** Hum. Reprod. 2016; 31: 844–853. https://doi.org/10.1093/humrep/dew008

Kyo, S., Nakamura, M., Kiyono, T., Maida, Y., Kanaya, T., Tanaka, M., Yatabe, N., Inoue, M. **Successful Immortalization of Endometrial Glandular Cells with Normal Structural and Functional Characteristics.** Am. J. Pathol. 2003; 163: 2259–2269. https://doi.org/10.1016/S0002-9440(10)63583-3

Li, J., Tibshirani, R. **Finding consistent patterns: A nonparametric approach for identifying differential expression in RNA-Seq data.** Stat. Methods Med. Res. 2011; 22: 519–536. https://doi.org/10.1177/0962280211428386

Livak, K.J., Schmittgen, T.D. **Analysis of relative gene expression data using real-time quantitative PCR and the 2-ΔΔCT method.** Methods 2001; 25: 402–408. https://doi.org/10.1006/meth.2001.1262

Masuda, A., Katoh, N., Nakabayashi, K., Kato, K., Sonoda, K., Kitade, M., Takeda, S., Hata, K., Tomikawa, J. **An improved method for isolation of epithelial and stromal cells from the human endometrium.** J. Reprod. Dev. 2016; 62: 213–218. https://doi.org/10.1262/jrd.2015-137

Montesano, R., Matsumoto, K., Nakamura, T., Orci, L. **Identification of a fibroblast-derived epithelial morphogen as hepatocyte growth factor.** Cell 1991; 67: 901–908. https://doi.org/10.1016/0092-8674(91)90363-4

Noyes, R.W., Hertig, A.T., Rock, J. **Dating the Endometrial Biopsy.** Fertil. Steril. 1950; 1: 3–25. https://doi.org/10.1016/S0015-0282(16)30062-0

Psychoyos, A. **Uterine Receptivity for Nidation.** Ann. N. Y. Acad. Sci. 1986; 476: 36–42. https://doi.org/10.1111/j.1749-6632.1986.tb20920.x

Rubin, J.S., Chan, A.M., Bottaro, D.P., Burgess, W.H., Taylor, W.G., Cech, A.C., Hirschfield, D.W., Wong, J., Miki, T., Finch, P.W. **A broad-spectrum human lung fibroblast-derived mitogen is a variant of hepatocyte growth factor.** Proc. Natl. Acad. Sci. U. S. A. 1991; 88: 415–419. https://doi.org/10.1073/pnas.88.2.415

Schindelin, J., Arganda-Carreras, I., Frise, E., Kaynig, V., Longair, M., Pietzsch, T., Preibisch, S., Rueden, C., Saalfeld, S., Schmid, B., Tinevez, J.Y., White, D.J., Hartenstein, V., Eliceiri, K., Tomancak, P., Cardona, A. **Fiji: An open-source platform for biological-image analysis.** Nat. Methods 2012; 9: 676–682. https://doi.org/10.1038/nmeth.2019

Sha, A.G., Liu, J.L., Jiang, X.M., Ren, J.Z., Ma, C.H., Lei, W., Su, R.W., Yang, Z.M. **Genome-wide identification of micro-ribonucleic acids associated with human endometrial receptivity in natural and stimulated cycles by deep sequencing.** Fertil. Steril. 2011; 96. https://doi.org/10.1016/j.fertnstert.2011.04.072

Talbi, S., Hamilton, A.E., Vo, K.C., Tulac, S., Overgaard, M.T., Dosiou, C., Le Shay, N., Nezhat, C.N., Kempson, R., Lessey, B.A., Nayak, N.R., Giudice, L.C. **Molecular phenotyping of human endometrium distinguishes menstrual cycle phases and underlying biological processes in normo-ovulatory women.** Endocrinology 2006; 147: 1097–1121. https://doi.org/10.1210/en.2005-1076

Thathiah, A., Carson, D.D. **Mucins and blastocyst attachment.** Rev. Endocr. Metab. Disord. 2002; 3: 87–96. https://doi.org/10.1023/A:1015446626671

Zheng, F., Yu, H., Lu, J. **High expression of MUC20 drives tumorigenesis and predicts poor survival in endometrial cancer.** J. Cell. Biochem. 2019: 1–8. https://doi.org/10.1002/jcb.28466

Received 20 January 2019; received in revised form 20 April 2019; accepted 8 May 2019.